

# Advanced Receiver Autonomous Integrity Monitoring Using Triple Frequency Data with a Focus on Treatment of Biases

Ahmed El-Mowafy

*Department of Spatial Sciences, Curtin University, Australia*

Email: a.el-mowafy@curtin.edu.au

## Abstract

Most current Advanced Receiver Autonomous Integrity Monitoring (ARAIM) methods are designed to use dual-frequency ionosphere-free observations. These methods assume that receiver bias is absorbed in the common receiver clock offset and bound satellite biases by nominal values. However, most multi-constellation Global Navigation Satellite Systems (GNSS) can offer triple frequency data that can be used for civilian applications in the future, which can improve observation redundancy, solution precision and detection of faults. In this contribution, we explore the use of this type of observations from GPS, Galileo and BeiDou in ARAIM. Nevertheless, the use of triple frequency data introduces receiver differential biases that have to be taken into consideration. To demonstrate the significance of these additional biases we first present a method to quantify them at stations of known coordinates and using available products from the International GNSS service (IGS). To deal with the additional receiver biases, we use a between-satellite single difference (BSSD) observation model that eliminates their effect. A pilot test was performed to evaluate ARAIM availability for Localizer Performance with Vertical guidance down to 200 feet (LPV-200) when using the triple-frequency observations. Real data were collected for one month at stations of known coordinates located in regions of different satellite coverage characteristics. The BSSD triple-frequency model was evaluated to give early indication about its feasibility, where the implementation phase still requires further comprehensive studies. The vertical position error was always found to be bounded by the protection level proven initial validity of the proposed integrity model.

*Keywords:* ARAIM; GNSS; Integrity Monitoring; biases; LPV-200.

## 1. Introduction

The presence of multiple GNSS constellations that provide a global coverage with multiple frequency observations led to the development of Advanced Receiver Autonomous Integrity Monitoring (ARAIM) methods for aircraft localizer performance with vertical guidance. For example, integration of GPS with Galileo in ARAIM has been shown in Rippl *et al.* (2011), and in Choi *et al.* (2012); Walter *et al.* (2013) using GPS and GLONASS. Integration of GPS with BeiDou in ARAIM has been demonstrated in Lijun *et al.* (2012); Liu and Zhu (2014); and El-Mowafy (2016).

The current proposed ARAIM methods use dual-frequency observations. Nevertheless, Galileo, BeiDou and GPS block III satellites provide triple-frequency observations. The additional use of a third frequency can improve positioning accuracy compared to the dual-frequency case (Elsobeiey, 2015; Duong *et al.*, 2016) and can enhance the fault detection

capability (Guo et al., 2011), which is a fundamental task in integrity monitoring. Another advantage of the use of a third frequency is that in case of unavailability of observation from one frequency, the remaining data of the satellite can still be used without excluding this satellite. Nevertheless, aviation requires the use of signals operating in designated safety-of-life aeronautical radionavigation service (ARNS) band. At present, the International Civil Aviation Organisation (ICAO) has not published the required navigation standards for Galileo and BeiDou, and the standards for dual-frequency use. However, these standards are expected to be available in the near future. Naturally, the implementation phase of a third frequency still requires a long road until the three signals are operationally available and regulations and policies are developed.

Although the use of multi-constellation GNSS signals can enhance positioning accuracy and integrity monitoring (IM), such improvement requires proper handling and bounding of biases not only for satellite observations from each constellation but also among different constellations. The observation biases are dependent on the receiver and the individual satellite signal characteristics. They are mainly caused by signal distortion in the analogue and digital parts of the signal chain, which produces distortions in the chip shape that cause the receiver's correlation function to deviate from its ideal triangular shape leading to a shift in the tracking point, and thus causes a bias in the measured pseudorange (Hauschild and Montenbruck, 2016). Additional biases are attributed to satellite orbit and clock navigation message miss-modelling, antenna phase centre offsets, inter-frequency biases, code-carrier incoherence, in addition to signal path through the antenna, splitter, cabling and amplifier (Phelts, 2007). It is typically assumed that the signal characteristics of the satellites from the same GNSS constellation on the same spectral band are identical. Hence, in the current ARAIM dual-frequency methods, the receiver biases are assumed absorbed into the common receiver clock offset and the satellite biases are bounded by a nominal value. However, differential receiver biases will be introduced when a third civilian frequency is used due to the fact that receiver biases are frequency dependent, which then require a proper treatment.

In this paper, we explore the feasibility of using a third frequency in ARAIM by creating two dual frequencies ionosphere-free (*IF*) observations, expecting the presence of these signals for civilian use in the future. To this end, instead of making assumptions on the differential receiver biases between the two *IF* observations, or trying to estimate them, where both approaches have a degree of uncertainty, we use a between-satellite single difference (BSSD) observation model in place of the traditional undifferenced observation model. This approach eliminates receiver clock offset as well as receiver hardware biases and therefore solves the problem at hand.

In the following sections, integrity monitoring using the triple-frequency data is presented. A method for estimation of biases at stations of known coordinates is discussed to show the significance of the differential code biases and that they should be considered when using triple frequency observations. The implementation of the BSSD model in ARAIM using triple-frequency data to cancel these biases is next discussed. Then, results of experimental evaluation of ARAIM availability is presented and analyzed at representative sites using data from multiple-constellations, including GPS, Galileo and BeiDou.

## 2. The triple-frequency observation model

In this study we use triple frequency data in the form of two ionosphere-free (*IF*) combinations. The *IF* observation equation of the pseudorange code measurements for satellite  $m$  from a GNSS constellation, such as Galileo, to receiver  $r$  for signals  $c_i$  and  $c_j$  on frequencies  $f_i$  and  $f_j$  in length units can be expressed as (El-Mowafy, 2014):

$$p(IF_{c_{i,j}})_r^m = \rho_r^m + C(dt_{\check{r}} - dt^m) + T^m + C d^m(IF_{c_{i,j}}) + \varepsilon_{P(IF_{c_{i,j}})_r^m} \quad (1)$$

where

$$dt_{\check{r}} = dt_r + d_r(IF_{c_{i,j}}), \quad d_r(IF_{c_{i,j}}) = a_{i,j} d_r(c_i) - b_{i,j} d_r(c_j) \quad (2)$$

$$d^m(IF_{c_{i,j}}) = a_{i,j} d^m(c_i) - b_{i,j} d^m(c_j) \quad (3)$$

$$\text{with } a_{i,j} = \frac{f_i^2}{f_i^2 - f_j^2}, \quad b_{i,j} = \frac{f_j^2}{f_i^2 - f_j^2} \quad (4)$$

$p(c_j)_r^m$  is the ionosphere-free combination code measurements,  $\rho_r^m$  is the satellite-to-receiver range,  $C$  is the speed of light in vacuum,  $dt_r$  and  $dt^m$  are the receiver and satellite clock offsets.  $T^m$  is the troposphere delay,  $\varepsilon_{P(c_j)_r^m}$  comprises measurement noise and multipath of code measurements.  $d_r(c_i)$  and  $d^m(c_i)$  are the receiver and satellite hardware biases for  $c_i$  in time units, and similarly  $d_r(c_j)$  and  $d^m(c_j)$  for  $c_j$ . It is typically assumed that the signal characteristics of the satellites from the same GNSS constellation on the same spectral occupation are identical. Hence, it follows that the receiver-dependent biases are assumed the same for all observations modulated on the same frequency for all satellites from the same constellation. Thus, in the above model, the receiver hardware bias is combined with the common receiver clock offset, and the joint term  $dt_{\check{r}}$  is determined as one of the unknowns per constellation.

In the case of using triple-frequency data, for instance using  $c_k$  in addition to  $c_i$  and  $c_j$ , a second *IF* observation is added to Eq. (1), such that:

$$p(IF_{c_{i,k}})_r^m = \rho_r^m + C(dt_{\check{r}} - dt^m) + T^m + C d^m(IF_{c_{i,k}}) + \Delta d_r(IF_{c_{i,j}}, IF_{c_{i,k}}) + \varepsilon_{P(IF_{c_{i,k}})_r^m} \quad (5)$$

where

$$\Delta d_r(IF_{c_{i,j}}, IF_{c_{i,k}}) = d_r(IF_{c_{i,k}}) - d_r(IF_{c_{i,j}}) \quad (6)$$

is a receiver differential code bias (DCB). This term appears because a common receiver clock offset is used for all frequency combinations whereas it includes the bias of the ionosphere-free combination of the first pair of observations ( $i, j$ ) as shown in (2). Hence, when the third frequency  $k$  is used; the additional differential receiver bias  $\Delta d_r(IF_{c_{i,j}}, IF_{c_{i,k}})$  needs to be considered and bounded. Furthermore, when combining measurements from different constellations, as usually is the case in ARAIM, and when computing the vertical protection

levels ( $PL$ ), which includes an overbounding term for satellite biases, receiver biases among different constellations have to be taken into consideration.

### 3. Receiver DCBs due to the use of a third frequency

To demonstrate the significance of the DCBs when using two IF combinations of triple-frequency data, we estimate in this section the DCBs at IGS stations of known coordinates and using available IGS products. Note here that this estimation method of DCBs is not a part of the proposed ARAIM approach.

Let us first re-parameterize the  $IF$  combination of phase observations for  $c_i$  and  $c_j$  in the form:

$$\phi(IF_{c_{i,j}})_r^m = \tilde{\rho}_r^m + M^m(IF_{c_{i,j}}) + \varepsilon_{P(IF_{c_{i,j}})_r^m} \quad (7)$$

where

$$\tilde{\rho}_r^m = \rho_r^m + C(dt_r - dt^m) + T^m \quad (8)$$

and  $M^m$  denotes the phase ambiguities.

The first step to estimate the code biases is to determine  $\tilde{\rho}_r^m$ . Since point positions are known at the test IGS stations, one can determine the phase ambiguities using for instance the Least-squares Ambiguity Decorrelation Approach (LAMBDA) (Teunissen, 1999). By substituting the estimated values of  $M^m(IF_{c_i,c_j})$  in (8) and ignoring phase noise and biases, which are very small in magnitude compared with the corresponding code terms - typically at a few mm,  $\tilde{\rho}_r^m$  can be determined from:

$$\tilde{\rho}_r^m = \phi(c_j)_r^m + \mu_j I^m - M^m(c_j) \quad (9)$$

After re-arranging terms of (1), we have

$$p(IF_{c_{i,j}})_r^m = \tilde{\rho}_r^m + C\left(d_r(IF_{c_{i,j}}) - d^m(IF_{c_{i,j}})\right) + \varepsilon_{P(IF_{c_{i,j}})_r^m} \quad (10)$$

By substituting for the  $\tilde{\rho}_r^m$  determined from (9), the bias term  $C\left(d_r(IF_{c_{i,j}}) - d^m(IF_{c_{i,j}})\right)$  can be estimated from (10) after filtering out the noise and multipath by averaging the results over a relatively long period of time. This period is selected at each station such that to reduce the effect of multipath and noise, only observations from the central part of the satellite pass with elevation angles higher than  $40^\circ$  are used. From (10), the term  $d^m(IF_{c_{i,j}})$  can be estimated from the IGS-Multi-GNSS Experiment (MGEX) products (<http://igs.org/mgex/products>), as explained in El-Mowafy *et al.*, 2016, and finally,  $d_r(IF_{c_{i,j}})$  can be determined from:

$$C d_r(IF_{c_{i,j}}) = p(IF_{c_{i,j}})_r^m - \tilde{\rho}_r^m + C d^m(IF_{c_{i,j}})$$

Table 1 summarizes the estimated average values of the DCBs between two  $IF$  combinations  $\left(\Delta d_r\left(IF_{c_{i,j}}, IF_{c_{i,j}}\right)\right)$ , for GPS, Galileo and BeiDou satellites that have triple frequency observations. The  $IF$  combinations used were L1/L5 and L1/L2 for GPS, E1/E5a and E1/E5b for Galileo, and B1/B2 and B1/B3 for BeiDou. Note that L2 is given here only for demonstration purpose where in the GPS Block III other signals such as L1C and L2C will be available. The data used were collected over June 2016 at 16 IGS stations of a global distribution using the same receiver model (Trimble NetR 9). As the table shows,  $\Delta d_r\left(IF_{c_{i,j}}, IF_{c_{i,j}}\right)$  is more than 1.5 m for GPS and BeiDou and 0.14 m for Galileo, which are significant values that cannot be ignored. Furthermore, these differential biases are not constant and change between days. Therefore, allocating an overabounding value for the DCBs in the integrity model similar to the way that satellite biases are treated in the current ARAIM methods would require assigning a high value to cover a wide range of receiver models. This would result in an increase of the PL and hence a reduction of ARAIM availability. Therefore, eliminating these receiver DCB terms would be a better option, which will be discussed in the next section using the BSSD approach.

Table 1. Average receiver DCB between ionosphere-free combinations (m)

GPS L1/L5 - L1/L2	Galileo E1/E5a - E1/E5b	BeiDou B1/B2 - B1/B3
1.895	0.138	1.502

#### 4. Between-satellite single difference (BSSD) of triple observations model in ARAIM

In this study, triple-frequency BSSD model is presented restricting our focus to the integrity evaluation process. The fault detection and exclusion (FDE) process will be discussed in detail in a separate study.

##### 4.1. Integrity evaluation with a triple frequency BSSD model

The use of BSSD model for measurements on the same frequency from the same constellation removes the receiver clock offset and eliminates the receiver-dependent differential hardware biases. For instance, by differencing the measurements from satellite  $m_G$  with measurements from a pivot (reference) satellite, denoted as  $l_G$ , which can be chosen as the satellite with the largest elevation angle, the BSSD code observation for  $c_{i,j}$  is:

$$p(IF_{c_{i,j}})_r^{m,l} = \rho_r^{m,l} - C(dt^{m,l} + d(IF_{c_{i,j}})^{m,l}) + T^{m,l} + \varepsilon_{p(IF_{c_{i,j}})_r^{m,l}} \quad (11)$$

where  $\rho_r^{m,l}$  is the single-difference satellite-to-receiver range, which equals  $(\rho_r^l - \rho_r^m)$ ,  $d(IF_{c_{i,j}})^{m,l}$  is the between-satellite  $IF$  bias,  $T^{m,l}$  is the single difference troposphere delay  $(T^l - T^m)$ , and  $\varepsilon_{p(IF_{c_{i,j}})_r^{m,l}}$  is the BSSD code measurement noise. Similarly for the second  $IF$  observation  $c_{i,k}$  in the triple-frequency system, we have:

$$p(IF_{c_{i,k}})_r^{m,l} = \rho_r^{m,l} - C(dt^{m,l} + d(IF_{c_{i,k}})^{m,l}) + T^{m,l} + \varepsilon_{p(IF_{c_{i,k}})_r^{m,l}} \quad (12)$$

For one  $IF$  pair of observations (e.g.  $i$  and  $j$ ), the BSSD model does not change observation redundancy compared with the undifferenced model. For a single constellation with  $N$  satellites, a redundancy of  $(N-4)$  is available using the latter model. The number of observations using BSSD is  $(N-1)$  and the number of states reduces from 4 (3D position + receiver clock offset) to 3 by excluding the receiver clock offset. Thus, the redundancy remains  $(N-4)$ . While the use of triple-frequency data provides more observations, it does not add to satellite geometry information, and thus at least four satellites still need to be observed. Furthermore, when integrating multi-constellation GNSS, one may opt not to use a pivot satellite from one system (e.g. Galileo) to form BSSD with satellites from other systems. An independent receiver clock offset for each constellation will be needed, which will help in preventing errors in the pivot-satellite constellation from being transferred to other systems. Therefore, each system will have its own reference satellite and thus a minimum of two satellites are needed from each system to be useful.

For ARAIM, the BSSD linearized measurement model in a general form can be written as:

$$B y = G x + B A_f x_f + B b^{sat} + \varepsilon \quad (13)$$

where  $y$  is the measurement vector taken as the difference between the observed code measurements and the calculated ones from satellite coordinates and the approximate receiver coordinates, determined for instance by single point positioning of code measurements of one constellation, e.g. GPS.  $x$  denotes the difference between the final and approximate values of the unknown parameters, which only comprises the 3D position components.  $x_f$  is the fault (or large errors) state vector, which includes possible failures defined for instance in (Blanch *et al.*, 2013).  $A_f$  is used to characterize suspected faults, such that the number of its columns equals the number of suspected satellites in each fault mode. Each of the columns in  $A_f$  has a one in the index corresponding to the satellite assumed to be affected and zero elsewhere.  $b^{sat}$  is a vector of the satellite-related biases and  $\varepsilon$  is the BSSD noise vector. For one of the integrated systems, (e.g. GPS) with  $N$  observed satellites with two  $IF$  combinations for the triple frequency observations,  $B_{2(N-1) \times 2N} = [u_{2(N-1) \times 2} \quad -I_{2(N-1) \times 2(N-1)}]$ , where  $I$  is the identity matrix and the subscripts define dimension of the matrix,  $u_{2(N-1) \times 2} = (I_{2 \times 2})_{2(N-1)} = \begin{bmatrix} 1 & 0 & \dots & 1 & 0 \\ 0 & 1 & \dots & 0 & 1 \end{bmatrix}^T$ . For the combined constellations, e.g. starting from GPS and ending by BeiDou (BDS) with  $M$  observed satellites, the  $B$  matrix is:

$$B = \begin{bmatrix} B^G_{2(N-1) \times 2N} & \dots & 0_{2(N-1) \times 2M} \\ \vdots & \ddots & \vdots \\ 0_{2(M-1) \times 2N} & \dots & B^{BDS}_{2(M-1) \times 2M} \end{bmatrix} \quad (14)$$

where each system has its reference satellite,  $B^G$  and  $B^{BDS}$  are the B matrix for GPS and BDS.

The direction cosine matrix  $G$  provides the transformation between the observation domain and the position domain, such that for the BSSD between satellites  $m$  and  $l$ , the corresponding row of  $G$  for one pair of frequencies, i.e.  $G^{m,l}$  reads:

$$G^{m,l} = [-c\theta_m \alpha_m + c\theta_l \alpha_l \quad -c\theta_m \alpha_m + c\theta_l \alpha_l \quad -s\theta_m + s\theta_l] \quad (15)$$

where “ $c$ ” denotes the cosine, “ $s$ ” is the sin,  $\theta$  and  $\alpha$  are the elevation angle and azimuth of the satellite, which are determined from the broadcast satellite ephemeris and the approximate receiver position. The final  $G$  of the combined systems, with  $N$  to  $M$  observed satellites, is:

$$G = \begin{bmatrix} G_{2(N-1) \times 3} \\ \vdots \\ G_{2(M-1) \times 3} \end{bmatrix} \quad (16)$$

The covariance matrix in ARAIM includes the User Range Accuracy ( $URA$ ), changes in the troposphere delay, multipath and noise effects. The  $URA$  represents the standard deviation that bounds the stochastic changes in range related to satellite clock and ephemeris errors in the absence of faults and used to evaluate availability of integrity monitoring (El-Mowafy and Yang, 2016). The  $URA$  is broadcast in the navigation message and will be sent in the planned Integrity Support Message. For Galileo, the Signal-in-Space-Accuracy ( $SISA$ ) replaces  $URA$ . It is assumed that observations from each satellite are uncorrelated. A single user standard deviation ( $\sigma_{user}$ ) combines the multipath and noise effects, where some related models were suggested, for instance as a function of the satellite elevation angle as shown in RTCA (1991); Lee and McLaughlin (2007) and Blanch *et al.* (2015). To form the covariance matrix for the two  $IF$  combinations on the triple-frequencies  $i, j, k$ , let  $a = (\frac{f_i^2}{f_i^2 - f_j^2})^2$ ,  $b = (\frac{f_j^2}{f_i^2 - f_j^2})^2$ ,  $c = (\frac{f_i^2}{f_i^2 - f_k^2})^2$  and  $d = (\frac{f_k^2}{f_i^2 - f_k^2})^2$ , which gives for satellite  $s$ :

$$Q_{user_s} = \begin{bmatrix} a & b & 0 \\ c & 0 & d \end{bmatrix} \text{diag}(\sigma_{i,user}^2, \sigma_{j,user}^2, \sigma_{k,user}^2) \begin{bmatrix} a & b & 0 \\ c & 0 & d \end{bmatrix}^T \quad (17)$$

Accordingly, assuming that  $\sigma_{user}^2 = \sigma_{i,user}^2 = \sigma_{j,user}^2 = \sigma_{k,user}^2$ , the covariance matrix for integrity monitoring for satellite  $s$  (denoted as  $Q_{URAs}$ ) using two dual-frequency  $IF$  observations before applying the BSSD is expressed as:

$$Q_{URAs} = \sigma_{user}^2 \begin{bmatrix} a^2 + b^2 & a c \\ a c & c^2 + d^2 \end{bmatrix} + (URA_s^2 + \sigma_{tropo_s}^2) \begin{bmatrix} 1 & 1 \\ 1 & 1 \end{bmatrix} \quad (18)$$

where  $\sigma_{tropo}$  is the standard deviation for the troposphere delay. The  $URA$  and  $\sigma_{tropo}$  are the same for the two dual-frequency  $IF$  observations, giving a correlation coefficient=1, and thus covariance  $\approx URA^2$  and  $\sigma_{tropo}^2$ . For the combined system, the covariance matrix is  $Q_{URAsats} = \text{diag}(Q_{URA_1}, \dots, Q_{URA_N}; \dots Q_{URA_M})$  for satellites 1 to  $N$  of the first system, 1 to  $M$  in the second, etc. When applying the BSSD model, the corresponding covariance matrix (denoted as  $Q_{URA}$ ) is:

$$Q_{URA} = B Q_{URAsats} B^T \quad (19)$$

and the weight matrix ( $W_{URA}$ ) is computed as  $W_{URA} = Q_{URA}^{-1}$ .

The least square solution of the unknown parameters for all satellites in view is:

$$\hat{x} = S^T B y \quad (20)$$

where  $S^T = (G^T W_{URA} G)^{-1} G^T W_{URA}$  is the projection matrix from the observation domain to the position domain. The Multiple Hypothesis Solution Separation method (MHSS) is applied in this study. The MHSS evaluates different fault modes given the specified probabilities of faults and determines the optimal probability of missed detection (Blanch *et al.*, 2012; Joerger and Pervan, 2014). In MHSS, a position error bound is created for each fault mode by computing a position solution unaffected by the fault, computing an error bound around this solution and accounting for the difference between all-in-view position solution and the fault tolerant position. For instance, for fault mode  $i$ , which can represent one or multiple faulty satellites from one or more constellations,  $S_i$  is formed similar to  $S$  by excluding the suspected satellites where  $S_i^T = (G^T A_i W_{URA} G)^{-1} G^T A_i W_{URA}$ .  $A_i$  is an identity matrix where the diagonal elements corresponding to  $i$  are zeros. The position estimate corresponding to this mode is  $\hat{x}_i = S_i^T B y$ .

The LPV-200 requirements described in the ICAO (2009) GNSS standards and recommended practices (SARPs) that can be used for evaluation of ARAIM availability are:

- 4 m, 95% accuracy requirement;
- 10 m, 99.99999% (i.e.  $1-10^{-7}$ ) fault free vertical position error requirement,
- Effective Monitor Threshold (*EMT*) requirement  $\leq 15$  m, and
- $VPL \leq VAL$  requirement, where  $VPL$  is the vertical PL and  $VAL$  is the Vertical Alert Level, which equals 35m for LPV-200.

The last requirement is in the hazardous category and the other requirements are usually met when this requirement is encountered and therefore ARAIM can be considered practically available when  $VPL \leq VAL$ . In this contribution,  $VPL$  is computed following the baseline method presented in Blanch *et al.* (2014), as the  $\max\{VPL_o, \max(VPL_i)\}$ , where  $VPL_o$  is the  $VPL$  for the fault-free full set of available satellites computed as:

$$VPL_o = \text{Gaussian term} + \text{bias overbound} = K_{md,0} \times \sigma_{v,0} + |S_3^T| \times bias_{nom} \quad (21)$$

where  $|S_3^T|$  is the sum of elements of the third row of  $S^T$  corresponding to the vertical position component. The maximum nominal bias,  $bias_{nom}$ , is used to bound possible non-zero mean error distributions at the satellite end, where receiver biases are assumed cancelled using the BSSD model. For fault mode  $i$ ,  $VPL_i$  is:

$$VPL_i = T_i + K_{md,i} \times \sigma_{v,i} + |S_{i3}^T| \times bias_{nom} \quad (22)$$

with

$$T_i = K_{ffd,i} \times \sigma_{dv,i} + |(S - S_i)_3^T| \times bias_{nom} \quad (23)$$

where  $\sigma_{v,0} = \sqrt{e_3^T S^T W_{URA}^{-1} S e_3}$  and  $\sigma_{v,i} = \sqrt{e_3^T S_i^T W_{URA}^{-1} S_i e_3}$ .  $e_3$  denotes a column vector whose 3<sup>rd</sup> entry is one and zero for the other entries.  $K_{md,0}$ ,  $K_{md,i}$  and  $K_{ffd,i}$  are scalar factors that are used to satisfy the miss-detection and false alert probabilities and are computed from the inverse of the complement of the one-sided standard normal cumulative distribution function.  $\sigma_{dv,i}$  is the standard deviation computed from:

$$\sigma_{dv,i} = \sqrt{e_3^T (S - S_i)^T W_{URE}^{-1} (S - S_i) e_3} \quad (24)$$

where  $W_{URE}$  is a weight matrix structured similar to  $W_{URA}$  by replacing the  $URA$  by the user range error ( $URE$ ) in (17). The  $URE$  is the non-integrity-assured standard deviation of the range component of satellite clock and ephemeris errors and is used to evaluate accuracy and continuity performance. For Galileo, the Signal-in-Space-Error ( $SISE$ ) replaces the  $URE$ .

#### 4.2. A note on modelling satellite biases using the BSSD model

In the BSSD model, the satellite nominal biases remained in Eqs. 21-23 after elimination of the receiver biases. For example between the satellites  $l$  and  $m$ , the satellite-related nominal bounding bias is  $bias_{nom}^{m,l} = bias_{nom}^l - bias_{nom}^m$ . This form has two contradictory effects on the computation of the PL, eventually almost balancing each other. On one hand, since in the MHSS the sign of the satellite biases are assumed unknown, to bound the biases and to ensure that the continuity requirement is met regardless of their actual signs, a conservative approach is to assume opposite signs for  $bias_{nom}^l$  and  $bias_{nom}^m$  when computing their difference. Accordingly, the maximum difference between two nominal satellite biases would be twice as much as that of a single satellite nominal bias, taking the same value of the nominal biases for all satellites from the same constellation. However, in practice biases have positive and negative signs. This is depicted in Figure 3, where the sign and value of the satellite biases on 04/07/2016 are illustrated for two  $IF$  observations forming possible triple frequency observations for block IIF GPS satellites and operational Galileo and BeiDou satellites. Hence, the difference between the observations of two satellites in the BSSD, for many satellites, will yield in practice a reduced bias effect whereas an overconservative PL is used.

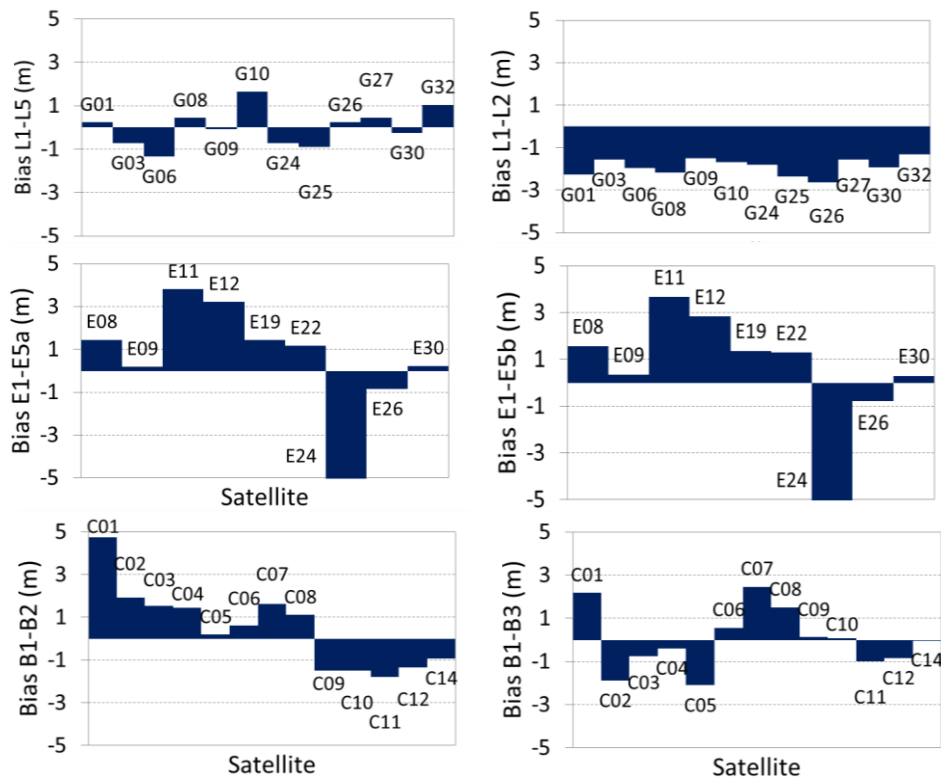


Fig. 3 Satellite biases for block IIF GPS satellites (L1/L5, L1/L2, top panel); Galileo (E1/E5a, E1/E5b, middle panel); BeiDou (B1/B2, B1/B3, bottom panel) on 4 July 2016.

On the other hand, the nominal biases are projected on the position domain using  $|S_3^T|$ ,  $|S_{i_3}^T|$ , and  $|(S - S_i)_3^T|$ . These projection (scaling) factors vary according to geometry of satellites and are significantly smaller in the BSSD model than their corresponding terms when using the un-differenced observation model (i.e. without applying BSSD) due to the use of differenced observations in the BSSD.

For numerical demonstration, Table 2 shows as an example the values of  $|S_3^T|$  and  $|S_{i_3}^T|$  in the two cases of using the undifferenced and BSSD observation models for one pair of dual-frequency observations for the first epoch of GPS data collected at station ZIM3 (which will be described later in the next section). For simplicity of presentation, the projection factors are only shown for testing the hypothesis of a single faulty satellite. The given  $|S_{i_3}^T|$  values are computed by eliminating the same satellites, defined in the table by their PRNs, when determining  $VPL_i$  in the undifferenced and BSSD observations. In both cases, 7 satellites were considered (PRNs 21, 8, 27, 16, 31, 18 and 29), where for BSSD PRN 21 was taken as the reference satellite. To compute  $VPL_i$ , one satellite was excluded in each run and the same 6 satellites were used when comparing results of the un-differenced and BSSD models. For example, when excluding PRN 8 satellites PRNs 21, 27, 16, 31, 18 and 29 were used in the undifferenced mode. For BSSD, the same satellites were used forming the differenced observation pairs 21-27, 21-16, 21-31, 21-18 and 21-29, which gives the same satellite geometry. One can notice the significant reduction of the projection factors in the BSSD case, which was 50-60% of the undifferenced case.

Eventually, the difference in the impact of the bounding approach of satellite biases between using the BSSD model and the un-differenced model will depend on the magnitude of the difference between the projection factor and the assumed amplification of the satellite bias. For the triple-frequency model, the same effect is experienced, where there are two  $S_3^T$  coefficients per satellite, which have the same value for the two  $IF$  observations if the same  $\sigma_{user}$  is used.

Table 2. Comparison of the projection factors in one epoch between using the conventional (un-differenced) and the BSSD models for one pair of dual-frequency observations

	$ S_3^T $	$ S_{i_3}^T $						
		Excluded PRNs	8	27	16	31	18	29
un-differenced observations	<b>4.09</b>		<b>4.09</b>	<b>4.36</b>	<b>4.01</b>	<b>3.89</b>	<b>4.10</b>	<b>7.36</b>
BSSD	<b>2.92</b>		<b>2.02</b>	<b>2.43</b>	<b>2.08</b>	<b>2.01</b>	<b>2.16</b>	<b>5.69</b>

## 5. Testing

In this section, a pilot experiment was carried out to evaluate performance of the triple frequency observations using the BSSD model in ARAIM. At the time of the test, there were 31 GPS satellites, 20 BeiDou satellites and 12 satellites in Galileo. Their full constellations will be operational within a few years. The test gives an initial indication about possible future performance.

### 5.1. Test description

The test data in our study covered June 2016 and include combined GPS, Galileo and BeiDou measurements collected at 65 IGS stations of known coordinates that have a global distribution (Dow et al., 2009). The receivers at these stations are capable of tracking all GNSS constellations with 30 seconds sampling rate. Real data were used in the test for the following reasons:

- i) to allow for the determination of the vertical position error (*VPE*), which is the difference between the known station vertical position and the computed one from real observations. When ARAIM availability requirement is met (i.e.  $VPL < VAL$ ), we check that *VPE* is bounded by the *VPL* as an indicator of the validity of the integrity model. This only offers a limited, albeit fundamental, check as the data used covered a limited period of time whereas an optimal test would need years of data to check the  $10^{-7}$  LPV-200 requirement.
- ii) To allow for the use of actual *URA* received via the satellite broadcast navigation data.

The number of observed satellites and their geometry, which are dependent on time of observation and station location, have a direct impact on the magnitude of the *VPL* and hence on ARAIM availability. Although at present, Galileo and BeiDou have partial constellations; testing using real data helps in resembling locations of constrained satellite visibility. In this section, we highlight results at selected representative sites for demonstration of the expected performance rather than showing results on a global scale. The three IGS stations; CUT0 (Australia), ZIM3 (Switzerland) and CPVG (Cape Verde) that represent three geographic regions were selected for this demonstration. Station CUT0 is located in Western Australia in the southern hemisphere, representing an area with good coverage by all constellations including all BeiDou satellites. Station CPVG in the Atlantic Ocean has an excellent coverage by GPS but poor coverage by BeiDou. Station ZIM3 is located in-between the two stations in Switzerland, with a partial coverage by BeiDou. The following symbols were used; GAL for Galileo and BDS for BeiDou.

The triple-frequency data used in the test included L1, L5 and L2 for GPS (where L2 was used for demonstration only); E1, E5a and E5b for GAL; and B1, B2 and B3 for BDS. They form two dual-frequency combinations for each system; which comprise L1/L5 and L1/L2 for GPS; E1/E5a and E1/E5b for GAL; and B1/B2 and B1/B3 for BDS. The data was available for Galileo and BeiDou, but since only block II-F satellites have L5, we simulated the L5 data for satellites from the blocks IIR and IIR-M. In the upcoming GPS Block III satellites, the future L1C and L2C signals may be used.

### 5.2. Used parameters in the error model

Knowledge of the stochastic characteristics of the signals is required in the error models used in ARAIM. Stochastic characteristics of GPS and Galileo observations were comprehensively discussed in the literature. For BeiDou, such studies are somewhat limited, e.g. Montenbruck et al. (2013); El-Mowafy and Hu (2014). Furthermore, while GPS and Galileo have medium Earth orbit (MEO) satellites, BeiDou additionally has Geostationary (GEO) and Inclined Geosynchronous Orbit (IGSO) satellites, which require a special modelling as shown in El-Mowafy and Hu (2014). Today, the minimum broadcast *URA* for GPS is 2.4 m but smaller values will become possible in the future when the new GPS CNAV message format is implemented for all satellites. BeiDou utilizes the same *URA* indexing system applied in GPS. CSNO, 2013 (<http://www.beidou.gov.cn/>) indicates that BeiDou *SIS* accuracy is  $\leq 2.5$  m and most current

navigation data of BeiDou gives a  $URA$  index of 0, i.e.  $URA \approx 2.4$  m. A formula is also given for its computation, where  $URA=2^{IN/2+1} \approx 2$  m for an index ( $IN$ ) = 0 (CSNO, 2013, aka).

A nominal satellite bias ( $Bias_{nom}$ ) of 0.75 m was assumed for all systems. For the  $URE$ , we assumed 0.5 m for GPS and 0.67 m for Galileo  $SISE$ . The  $URE$  reference values of MEO and IGSO satellites of BeiDou system were assumed similar to those of GPS. For GEO satellites, the  $URE$  index reference value was taken equals to an amplification ratio of the value given to the MEO satellites (Lijun *et al.*, 2012). A satellite elevation mask angle of 10 degrees was used to allow for small banking of aircraft. The a-priori probability for the single satellite fault ( $P_{sat}$ ) and constellation-wide faults ( $P_{const}$ ) for the systems GPS, BeiDou and Galileo are discussed in Blanch *et al.*, (2012); Walter *et al.* (2013); Rippl *et al.* (2014) and El-Mowafy (2013, 2016). We used here  $P_{sat}$  of  $10^{-5}$  for GPS and Galileo satellites and a conservative value of  $10^{-4}$  for BeiDou (El-Mowafy, 2013). A  $P_{const}$  equals  $10^{-4}$  was used for all constellations. Although these assumptions require further refinement, they are however sufficient for the purpose of this study.

The used model standard deviations include  $\sigma_{user} = \sqrt{\sigma_{mp}^2 + \sigma_{noise}^2}$  where (Blanch *et al.*, 2015):

$$\text{for multipath: } \sigma_{mp} = 0.13 + 0.53 e^{-\theta/10^\circ} \text{ (m)} \quad (25)$$

$$\text{for the noise: } \sigma_{noise} = 0.15 + 0.43 e^{-\theta/6.9^\circ} \text{ (m)} \quad (26)$$

$$\text{and for the troposphere: } \sigma_{tropo} = 0.12 \times \frac{1.001}{\sqrt{0.002001 + (\sin(\frac{\pi\theta}{180}))^2}} \text{ (m)} \quad (27)$$

### 5.3. Discussion of results

To demonstrate the initial validity of the proposed triple-frequency BSSD model, Table 3 shows the ratio of time ARAIM was available to the whole test period using current and possible future values (1m) of  $URA$  over June 2016. Figure 4 shows as an example the time series of the  $VPL$ , the absolute values of  $VPE$  and the  $VAL$  (35 m for LPV-200) on 19<sup>th</sup> June 2016 using the latter  $URA$ . The triple-frequency BSSD model was used at the three stations CUT0, ZIM3 and CPVG. Three cases were illustrated. In the first case, the three constellations were combined (top panel of Figure 4). In the second case, GPS was integrated with BeiDou (middle panel), and in the third case, GPS was combined with Galileo (bottom panel of the figure). The  $VPL$  values shown in the figure reflect the number of satellites available in each constellation as well as quality of the observations. Recall that for ARAIM to be available, the condition  $VPL \leq VAL$  should be met. From test results one can conclude the following:

- In all cases (where real data was used) the computed  $VPE$  was bounded by the  $VPL$  and  $VAL$  and thus no hazardous situation was encountered proven initial validity of the model. The  $VPE/VPL$  ratio was in general within  $\pm 0.25$ . The standard deviations of the  $VPE$  using the integrated constellations decreased as more constellations were added. The amount of improvement varied across the test sites according to number and quality of the collected observations. Furthermore, in almost all processed epochs, the outcome of the two ARAIM metrics, i.e. 95% and 99.99999% accuracy, follow the results of the requirement  $VPL \leq VAL$ .
- Table 3 shows the overall ARAIM availability using the broadcast values of  $URA$  as well as the availability with a hypothetical future  $URA$  that may reach 1 m, which is expected with the ongoing improvements in satellite orbit estimation, clock stability and the use of CNAV. The

table shows that even with current constellations, resembling sites with constrained satellite visibility, the use of this optimistic value of *URA* will give improved availability.

- The use of two constellations is almost sufficient to achieve a desired ARAIM availability when all constellations are operational with future expected values of *URA*. This is evident from the results at station CUT0 where a large number of satellites was observed from all constellations. In contrast, at station CPVG the current number of satellites of Galileo and BeiDou (particularly BeiDou) is limited which adds little to GPS. This situation will improve with time as more satellites being deployed until completion of the systems. These results agree with the predicted results published in the literature (EU-U.S. WG-C ARAIM, 2015, [www.gps.gov/policy/cooperation/europe/2015/working-group-c/ARAIM-milestone-2-report.pdf](http://www.gps.gov/policy/cooperation/europe/2015/working-group-c/ARAIM-milestone-2-report.pdf)).
- For the purpose of comparison with dual-frequency data, Table 4 shows the percentage of ARAIM availability when using dual-frequency observations (L1/L5 for GPS; E1/E5a for GAL; and B1/B2 for BDS) for the case of using a possible value of 1m *URA*, which is of more interest for future implementation of ARAIM. When comparing the Tables 3 and 4, one can see that the ARAIM availability was analogous for the two cases with some improvement using the triple-frequency data at station CPVG using GPS and BeiDou observations, which has a constrained BeiDou satellite view.
- Table 5 shows the positioning accuracy over June 2016 when comparing triple frequency-observations and the dual-frequency observations mentioned above for each combination of constellations at the three sites. The average of the absolute values of *VPE* is given as an indicator of the positioning accuracy. Overall, the improvement in the triple-frequency case due to the use of more observations albeit with the same satellite geometry when compared with using dual-frequency observations was less than 5%, except for two cases at ZIM3 and CPVG using GPS+BeiDou observations, which was marginally negative. This indicates that an updated modelling of the characteristics of BeiDou observations is required, particularly in conjunction with modernisation of the system and availability of BeiDou Block 3 satellites.

Table 3. Percentage of ARAIM Availability using triple-frequency data over June 2016

Constellations	CUT0		ZIM3		CPVG	
	Broad-cast <i>URA</i>	1m <i>URA</i>	Broad-cast <i>URA</i>	1m <i>URA</i>	Broad-cast <i>URA</i>	1m <i>URA</i>
GPS+GLN+BDS	100.00	100.00	96.66	100.00	95.05	100.00
GPS+ BDS	100.00	100.00	95.51	100.00	90.60	99.9999
GPS+ GAL	95.67	100.00	95.42	100.00	93.14	100.00

Table 4. Percentage of ARAIM Availability using dual-frequency data (1m *URA*)

Constellations	CUT0	ZIM3	CPVG
GPS+GLN+BDS	100.00	100.00	100.00
GPS+ BDS	100.00	100.00	97.980
GPS+ GAL	100.00	100.00	100.00

Table 5. Average of the absolute values of *VPE* using triple-frequency and dual-frequency observations over June 2016 with 1m *URA* (m)

Constellations	CUT0		ZIM3		CPVG	
	Triple-freq	Dual-freq	Triple-freq	Dual-freq	Triple-freq	Dual-freq
GPS+GLN+BDS	2.045	2.161	2.252	2.367	2.624	2.722
GPS+ BDS	2.160	2.197	2.506	2.421	2.943	2.878
GPS+ GAL	2.229	2.361	2.390	2.404	2.669	2.671

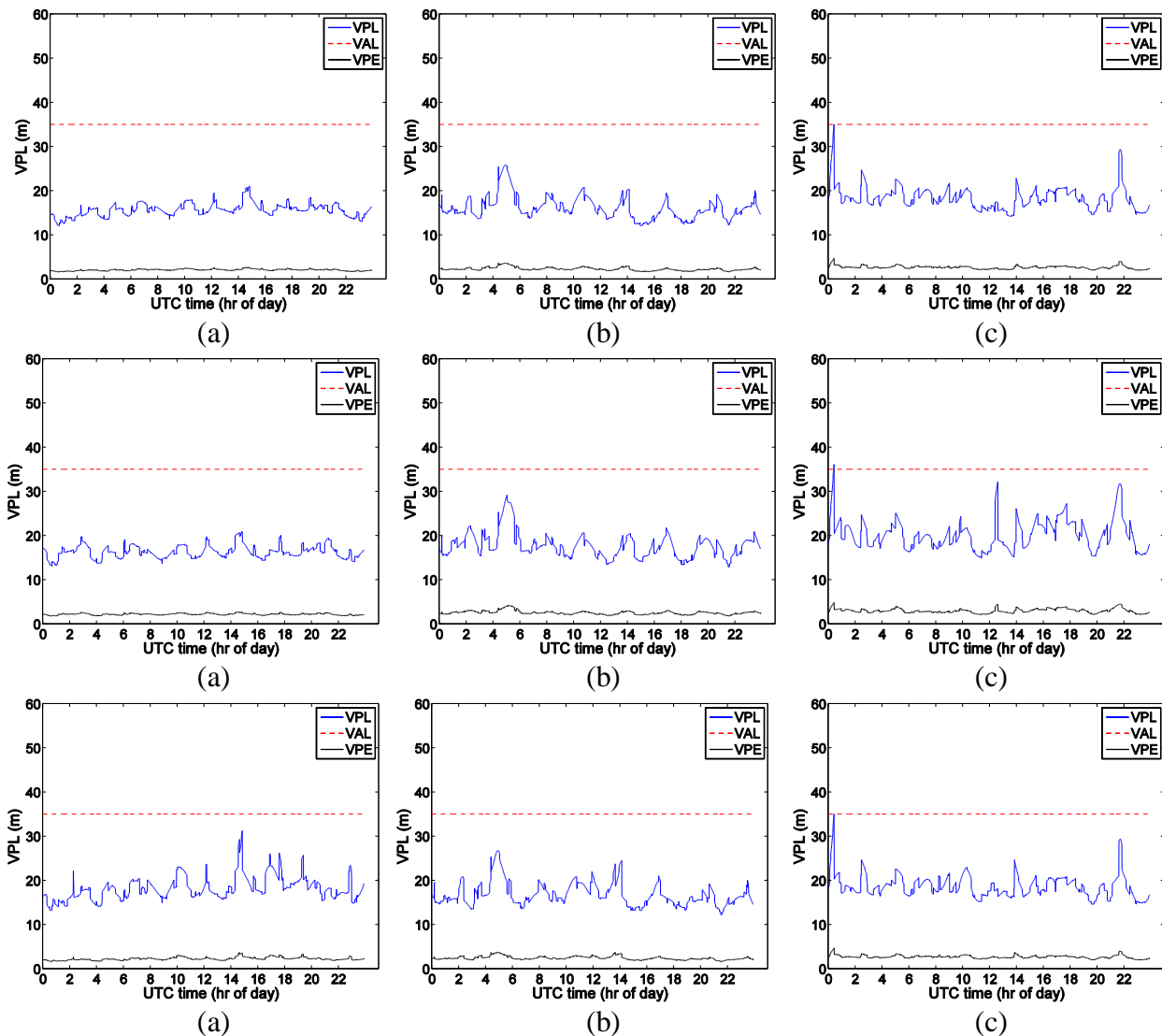


Fig. 4 Time series of *VPL* (1m *URA*) and *VPE* with *VAL* using triple-frequency observations; GPS +Galileo +BeiDou (top panel); GPS and BeiDou (middle panel) and GPS with Galileo (bottom panel) on 19<sup>th</sup> June 2016 at CUT0 (a), ZIM3 (b), and CPVG (C).

## 6. Conclusion

A pilot study on the feasibility of triple-frequency data for ARAIM is presented. In the current ARAIM dual-frequency methods, the receiver biases are assumed absorbed with the common receiver clock offset. However, with the use of a third frequency, significant receiver DCBs will appear since receiver biases are frequency dependent. Such DCBs are cancelled when BSSD observations are used. An ARAIM method implementing the BSSD approach is presented.

A pilot test was carried out to evaluate performance of using the triple-frequency observations from multiple constellations, including GPS, Galileo and BeiDou, when applying the proposed BSSD model in ARAIM. Results at regions of different satellite visibility characteristics prove the initial validity of the proposed model where in all cases, the *VPE* values were well bounded by the *VPL* during the test period. In agreement with the literature, with the ongoing improvements in satellite orbit estimation, clock stability and the use of CNAV, it is expected that a high degree of ARAIM availability will be achieved worldwide upon completion of all GNSS. The use of available triple-frequency observations when compared with dual-frequency data led to some improvement of ARAIM availability at sites with constrained satellite visibility and a small improvement of positioning accuracy.

## Acknowledgment

The Institute for Geoscience Research (TIGeR), Curtin University, is acknowledged for partially funding this research. The data used in this study was downloaded from the International GNSS Service (IGS) open-source streams. We would like to thank all providers of the data used.

## References

- Blanch, J., Walter, T., Enge, P., et al., 2012. Advanced RAIM User Algorithm Description: Integrity Support Message Processing, Fault Detection, Exclusion, and Protection Level Calculation, Proceedings of the 25th International Technical Meeting of The Institute of Navigation (ION GNSS 2012), Nashville, TN, September 2012, 2828- 849.
- Blanch, J., Walter, T., Enge, P., et al., 2013. Critical Elements for a Multi-Constellation Advanced RAIM. *Navigation*, 60(1): 53-69.
- Blanch, J., Walter, T., and Enge, P., 2014. Optimal Positioning for Advanced RAIM. *Navigation*, 60(4): 279-289.
- Blanch, J., Walter, T., Enge, P., et al., 2015. Baseline Advanced RAIM User Algorithm and Possible Improvements. *IEEE Transactions on Aerospace and Electronic Systems*, 51(1): 713:732.
- Choi, M., Blanch, J., Walter, T., et al., 2012. Evaluation of Multi-Constellation Advanced RAIM for Vertical Guidance using GPS and GLONASS Signals with Multiple Faults. Proceedings 25th International Technical Meeting, ION, Nashville TN, Sept. 17-21, 2012, 884-892.
- Dow, J.M., Neilan, R. E., and Rizos, C. 2009. The International GNSS Service in a changing landscape of Global Navigation Satellite Systems, *Journal of Geodesy*, 83,191–198.
- Duong, V. et al. 2016. Performance of Precise Point Positioning using Current Triple-frequency GPS Measurements in Australia. Proceedings of the International Global Navigation Satellite Systems Association, IGSS Conference 2016, 6 – 8 December 2016, Sydney, 1-15.
- El-Mowafy, A., 2013. RAIM for Vertical Guidance Using GPS and Beidou, *J. of Global Positioning System*. 12(1), 28-37.
- El-Mowafy, A. 2014. GNSS Multi-frequency Receiver Single-Satellite Measurement Validation Method, *GPS Solutions*, 18, 553-561.
- El-Mowafy, A., and Hu, C., 2014. Validation of BeiDou Observations, *Journal of Applied Geodesy*. 8(2), 155–168.
- El-Mowafy, A., Deo, M., Rizos, C., 2016. On Biases in Precise Point Positioning with Multi-Constellation and Multi-Frequency GNSS Data. *Measurement Science and Technology*, 27(3), 035102.

- El-Mowafy, A., 2016. Pilot Evaluation of Integrating GLONASS, Galileo and BeiDou with GPS in ARAIM. *Artificial Satellites*, 51(1), 31-44.
- El-Mowafy, A. and Yang, C. 2016. Limited Sensitivity Analysis of ARAIM Availability for LPV-200 over Australia using Real Data. *Advances in Space Research*, 57(2), 659–670.
- Elsobeiey, M. 2015. Precise Point Positioning using Triple-Frequency GPS Measurements. *J of Navigation*. 68: 480–492.
- Guo, J., Lu, M. Cui, X., Feng Z., 2011. A New RAIM Algorithm for Triple-Frequency GNSS Receivers. *Proceedings of the 2011 International Technical Meeting of The ION, San Diego, CA, 24 – 26 January, 2011*, 271 – 278.
- Hauschild A., and Montenbruck O., 2016. A study on the dependency of GNSS pseudorange biases on correlator spacing, *GPS Solutions*, 20:159-171.
- ICAO, Annex 10, 2009. GNSS standards and recommended practices (SARPs). Section 3.7, Appendix B, and Attachment D, *Aeronautical Telecommunications*, Vol. 1 (Radio Navigation Aids), Amendment 84.
- Joerger, M., and Pervan, B., 2014. Solution Separation and Chi-Squared ARAIM for Fault Detection and Exclusion,” *Proceedings of IEEE/ION PLANS 2014, Monterey, CA, May 2014*, 294-307.
- Lee, C., and McLaughlin, M. 2007. Feasibility Analysis of RAIM to Provide LPV-200 Approaches with Future GPS, *Proceedings of the ION GNSS 2007, Fort Worth, TX, Sept. 25-28*, 2898-2910.
- Lijun, P., Kai, J., Xiaojun, D., Yan, Z., et al., 2012. Receiver Autonomous Integrity Monitoring Parameter Design and Analysis for Multi-Constellation Navigation. *Proceedings China Satellite Navigation Conference (CSNC 2012)*, Vol. 2, 2012, 15-28.
- Liu, Y., and Zhu, Y., 2014. Design and Performance Evaluation of Airspace-Ground Cooperative GPS/BeiDou Dual-constellation RAIM Algorithm. *Proceedings of the International Technical Meeting ION 2014, San Diego, CA, 27-29 Jan. 2014*, 127-136.
- Montenbruck, O., Hauschild, A., Steigenberger, P., et al., 2013. Initial assessment of the COMPASS/BeiDou-2 regional navigation satellite system, *GPS Solutions*, 17(2), 211-222.
- Phelts, R.E., 2007. Range Biases on Modernized GNSS Codes,” *European Navigation ConferIGSence GNSS/TimeNav*, 29, Geneva, Switzerland, May 29 – 1 June 2007, Accessed online April 2015.
- Rippl, M., Spletter, A., and Günter, C., 2011. Parametric Performance Study of Advanced Receiver Autonomous Integrity Monitoring (ARAIM) for Combined GNSS Constellations. *Proceedings of the International Technical Meeting of The ION, San Diego, California, 24-26 Jan. 2011*, 285-295 .
- Rippl, M., Martini, I., Belabbas, B, et al. 2014. ARAIM Operational Performance Tested in Flight, *Proceedings of ION ITM 2014, San Diego, CA, 27-29 Jan, 2014*, 601-615.
- RTCA Special Committee 159, RTCA/DO-229D. 1991. WAAS Minimum Operational Performance Specification (MOPS).
- Teunissen P.J.G, 1999. An optimality property of the integer least-squares estimator. *J of Geodesy*. 73(11):587–593.
- Walter, T., Blanch, J., Choi, M.J., et al., 2013. Incorporating GLONASS into Aviation RAIM Receivers. *Proceedings of the 2013 International Technical Meeting of the Institute of Navigation, San Diego, CA, 27-29 January, 2013*, 239-249.